

Electric-Field Breakdown of Absolute Negative Conductivity and Supersonic Streams in Two-Dimensional Electron Systems with Zero Resistance/Conductance States

V. Ryzhii* and A. Satou

Computer Solid State Physics Laboratory, University of Aizu, Aizu-Wakamatsu 965-8580, Japan

(Dated: January 7, 2022)

We calculate the current-voltage characteristic of a two-dimensional electron system (2DES) subjected to a magnetic field at strong electric fields. The interaction of electrons with piezoelectric acoustic phonons is considered as a major scattering mechanism governing the current-voltage characteristic. It is shown that at a sufficiently strong electric field corresponding to the Hall drift velocity exceeding the velocity of sound, the dissipative current exhibits an overshoot. The overshoot of the dissipative current can result in a breakdown of the absolute negative conductivity caused by microwave irradiation and, therefore, substantially effect the formation of the domain structures with the zero-resistance and zero-conductance states and supersonic electron streams.

PACS numbers: PACS numbers: 73.40.-c, 78.67.-n, 73.43.-f

Recently, two experimental groups [1, 2] have reported the observation of vanishing electrical resistance in two-dimensional electron systems (2DES's) subjected to a magnetic field and strong microwave radiation. The occurrence of the effect of the so-called zero-resistance (ZR) and zero-conductance (ZC) states [1, 2, 3] has been linked to the effect of absolute negative conductivity (ANC) when the dissipative dc conductivity $\sigma(E)$, determined by the dark conductivity $\sigma_d(E)$ and microwave photoconductivity $\sigma_{ph}(E)$, is negative [4, 5, 6]. As speculated, the mechanism of ANC responsible for the occurrence of ZR and ZC states is associated with the photon-assisted scattering of electrons on impurities [7, 8, 9, 10, 11], although alternative mechanisms, particularly the photon-assisted interaction of electrons with acoustic phonons, can be essential as well [12, 13, 14, 15]. It has long been shown [7, 8] that the photon-assisted impurity scattering can result in a negative dissipative photoconductivity $\sigma_{ph}(E)$ in the situations in question when the microwave frequency Ω somewhat exceeds the cyclotron frequency $\Omega_c = eH/mc$ or its harmonics. According to the calculations [7, 8], the dissipative microwave photoconductivity can be negative at sufficiently strong irradiation at $0 < \Omega - \Omega_c \lesssim eEL/\hbar, \Gamma/\hbar$. Here e and m are the electron charge and effective mass, respectively, c is the velocity of light, E and H are the electric and magnetic fields, $L = (\hbar/eH)^{1/2}$ is the quantum Larmor radius, Γ is the Landau level (LL) broadening, and \hbar is the Planck constant.

It is crucial for the explanations of ZR and ZC states, invoking the concept of ANC, in a 2DES with both the Hall bar and Corbino configurations that there is an electric field E_0 at which $\sigma(E_0) = 0$ [5, 6, 16, 17]. The modulus of the dissipative photoconductivity decreases with increasing electric field when the latter becomes sufficiently large [7, 8], namely, when $E > E_b = \max\{\hbar(\Omega - \Omega_c)/eL, \Gamma/eL\}$. Hence, one can expect that E_0 is deter-

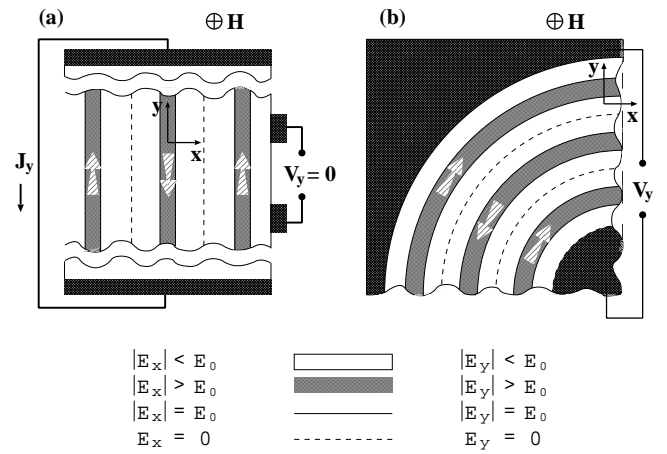


FIG. 1: Schematic view of possible domain structures in 2DES corresponding to (a) ZR states in the Hall bar configuration and input current (J_y is the input current and $V_y = 0$ is the measured voltage) and (b) ZC states in the Corbino geometry (here V_y is the applied voltage). Arrows show directions of the Hall current in different high-field domains.

mined by the resonance detuning and the LL broadening with $E_0 > E_b$. The characteristic field E_b is rather large. Indeed, at the magnetic field $H = 2$ kG, assuming that $|\Omega - \Omega_c|/\Omega_c = 0.25$, we have $E_b \simeq 20$ V/cm. The estimated values of E_b significantly exceed the average electric field $\langle E \rangle$ in the 2DES observed experimentally, which is in the range $\langle E \rangle \simeq 3 \times (10^{-3} - 10^{-1})$ V/cm depending on the sample geometry. Taking into account the instability of uniform electric-field distributions at $E < E_0$, one can conclude (see, for example, Refs. [5, 6, 11]), that in the case $\langle E \rangle \ll E_0$, nearly periodic domain structures are formed as shown in Fig. 1. In these domain structures, $|J_y| = \sigma_H d |\langle E_x \rangle| \ll \sigma_H d E_0$, $J_x = 0$, and $E_y = 0$ in the Hall bar configuration, and $|V_y| = d |\langle E_y \rangle| \ll d E_0$, $J_y = 0$, and $E_x = 0$ in the Corbino samples. Here σ_H is the Hall conductivity and d is the 2DES size. It would appear reasonable that the shape of the domains

*Electronic address: v-ryzhii@u-aizu.ac.jp

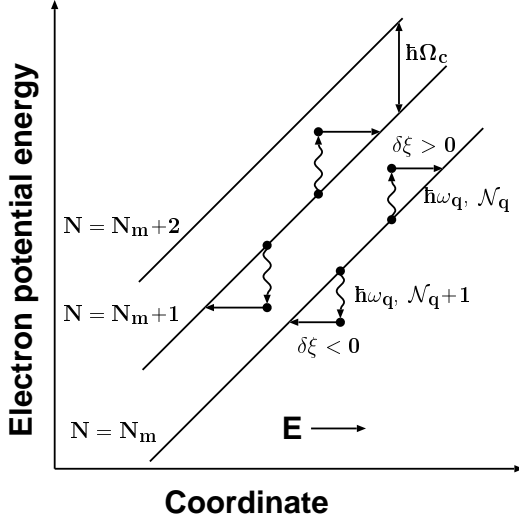


FIG. 2: Intra-LL electron transitions with absorption and emission of acoustic phonons and spatial shift of electron Landau centers $\delta\xi$.

and their parameters, in particular the swing of the electric field, depend on the behavior of the current-voltage characteristic, especially at $E \simeq E_0$. Thus, mechanisms providing ANC at low electric field are essential for the instability of uniform states that, as a matter of fact, result in the formation of the domains, whereas a mechanism providing the lowest value of E_0 can substantially govern the domain structure and, therefore, the observable macroscopic characteristics.

The electric-field dependence of the net dissipative conductivity can be determined not only by $\sigma_{ph}(E)$ but by $\sigma_d(E)$ as well. As shown in the following, the dark component can be a steep function of the electric field resulting in the breakdown of ANC if $\sigma_{ph}(E) < 0$. The contribution of the electron-impurity interaction to $\sigma_d(E)$ results in a smooth electric-field dependence up to very strong electric fields $E > E_c = \hbar\Omega_c/eL$ [18, 19, 20] (see also Ref. [11]). However, the contribution of the electron scattering on acoustic phonons, being fairly small at low temperatures and weak electric fields [13, 14, 21, 23], can lead to a sharp overshoot of the dissipative current (conductivity) at $E \simeq E_s = \hbar s/eL^2$, where s is the velocity of sound. The point is that at $E < E_s$, the selection rules allow only the electron-phonon scattering events accompanied by the inter-LL electron transitions. Since the energy of the acoustic phonons involved equals the LL separation $\hbar\Omega_c$, and therefore is rather large, the number of such phonons at low temperatures is exponentially small. This results in relatively small contribution of the electron-phonon interaction to the dissipative dark current (dissipative conductivity) at $E < E_s$. In contrast, at $E_s \lesssim E \ll E_c$, the intra-LL scattering transitions

can significantly contribute to the dissipative dark current. Such transitions are schematically shown in Fig. 2.

This range of the electric fields corresponds to the electron Hall drift velocity $v_H = cE/H \geq s$. Assuming $s = 3 \times 10^5$ cm/s and $H = 1 - 2$ kG, one can obtain $E_s \simeq 3 - 6$ V/cm. A peculiarity of the electron transport at $E \simeq E_s$ was pointed out previously, particularly in connection with the breakdown of the quantum Hall effect [21, 22, 23, 24, 25, 26, 27] (see also Refs. therein).

The dissipative dark current density $j_d(E)$ and, consequently, the dissipative dark conductivity $\sigma_d(E) = j_d/E$ of a 2DES in the case of the electron-phonon interactions can be calculated using the following formula:

$$j_d(E) = j_1 + j_2 = \sum_{N \neq N'} j_{N,N'} + \sum_N j_{N,N}, \quad (1)$$

where

$$j_{N,N'} = \frac{e}{\hbar} f_N (1 - f_{N'})$$

$$\times \int d^3\mathbf{q} q_y |V_{\mathbf{q}}|^2 |Q_{N,N'}(L^2 q_{\perp}^2/2)|^2$$

$$\times \{ \mathcal{N}_q \delta[(N - N')\hbar\Omega_c + \hbar\omega_q + eEL^2 q_y]$$

$$+ (\mathcal{N}_q + 1) \delta[(N - N')\hbar\Omega_c - \hbar\omega_q + eEL^2 q_y] \}. \quad (2)$$

Here f_N and \mathcal{N}_q , are the electron and phonon distribution functions, $N = 0, 1, 2, \dots$ is the LL index, $\mathbf{q} = (q_x, q_y, q_z)$, $\mathbf{q}_{\perp} = (q_x, q_y)$, and $\omega_q = sq$ are the phonon wave vector, its in-plane component, and the phonon frequency, respectively, $\delta(\omega)$ is the LL form-factor determined by Γ , $|V_{\mathbf{q}}|^2 = |C|^2 \exp(-l^2 q_z^2/2)/q$ describes the electron interaction with piezoelectric phonons, where l is the width of the electron localization in the z -direction perpendicular to the 2DES plane and $|C|^2$ is a constant. At a strong localization in the quantum well at the heterointerface, $l \ll L$. $|Q_{N,N'}(L^2 q_{\perp}^2/2)|^2 = |P_N^{N'-N}(L^2 q_{\perp}^2/2)|^2 \exp(-L^2 q_{\perp}^2/2)$ is determined by the overlap of the electron wave functions, and $|P_N^{N'-N}(L^2 q_{\perp}^2/2)|^2$ is proportional to a Laguerre polynomial $L_N^{N'-N}(L^2 q_{\perp}^2/2)$.

In the range of moderate electric fields (much smaller than E_c), the contribution of the electron scattering on acoustic phonons accompanied by the inter-LL transitions can be presented as [12]

$$j_1 \simeq \sigma_1 E, \quad (3)$$

$$\sigma_1 = \mu_1 \left(\frac{\hbar s}{TL} \right) \left(\frac{s}{L\Omega_c} \right) \exp\left(-\frac{\hbar\Omega_c}{T}\right) \exp\left(-\frac{l^2\Omega_c}{2s^2}\right), \quad (4)$$

where $\mu_1 \propto |C|^2 \sum_N f_N (1 - f_{N+1})/\sqrt{N}$ and T is the temperature (in energy units). The quantity j_1 remains

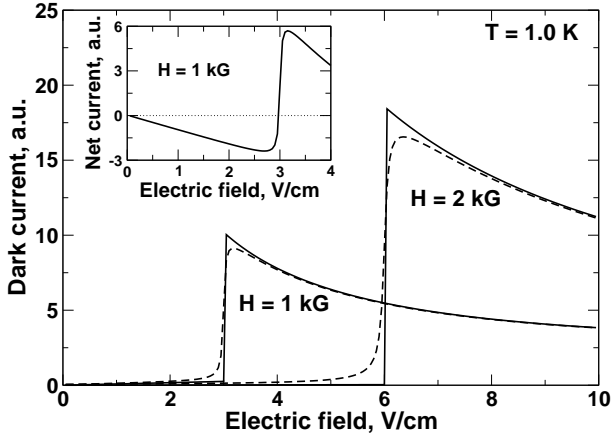


FIG. 3: Dissipative dark current-voltage characteristics for different magnetic fields. The dashed curve corresponds to the LL broadening $\Gamma/\hbar\Omega_c = 0.01$. Inset shows net current-voltage characteristic at microwave irradiation.

small up to very large electric fields [23] (as in the case of elastic impurity scattering [18, 20]) $E \simeq E_c$.

As for j_2 corresponding to the electron scattering on acoustic phonons accompanied by the intra-LL transitions, it equals zero at $E < E_s = \hbar s/eL^2$ because the scattering selection rule $\hbar\omega_q = eEL^2q_y$ is not met at low electric fields. At $E \geq E_s$, considering Eqs. (1) and (2), we obtain

$$j_2 = \frac{e|C|^2}{\hbar^2 s} \sum_N f_N(1 - f_N) \int d\Phi \sin \Phi dq_{\perp} \frac{q_{\perp}^2}{\sqrt{q^2 - q_{\perp}^2}} \times \exp(-l^2 q^2/2) \exp[(l^2 - L^2)q_{\perp}^2/2] |L_N^0(L^2 q_{\perp}^2/2)|^2 \times [\mathcal{N}_q \delta(q + Fq_{\perp} \sin \Phi) + (\mathcal{N}_q + 1) \delta(q - Fq_{\perp} \sin \Phi)]. \quad (5)$$

Here $F = eEL^2/\hbar s = cE/sH$ and $\sin \Phi = q_y/q_{\perp}$. In contrast to Ref. [25], we will focus on the case of large filling factors corresponding to the experimental conditions [1, 2, 3], i.e., the case $\zeta \gg \hbar\Omega_c$, where ζ is the Fermi energy reckoned from the lowest LL. In this case, the LL's with large N yield the main contribution (with $N = N_m$ and $N = N_m + 1$, where $\zeta/\hbar\Omega_c \leq N_m < \zeta/\hbar\Omega_c + 1$). When $N \gg 1$, $|L_N^0(L^2 q_{\perp}^2/2)|^2 \simeq J_0^2(\sqrt{2N}Lq_{\perp}) \simeq 2 \cos^2(\sqrt{2N}Lq_{\perp} - \pi/4)/\pi\sqrt{2N}Lq_{\perp}$, where $J_0(z)$ is the Bessel function. Taking this into account, after integrating over q Eq. (5) can be reduced to

$$j_2 = \frac{\mu_2 \hbar s}{2eL} \int d\Phi \sin \Phi dq_{\perp} \frac{\exp[-l^2(F^2 \sin^2 \Phi - 1)q_{\perp}^2/2]}{\sqrt{F^2 \sin^2 \Phi - 1}} \times \exp(-L^2 q_{\perp}^2/2) \cos^2[\sqrt{2N}Lq_{\perp} - \pi/4]. \quad (6)$$

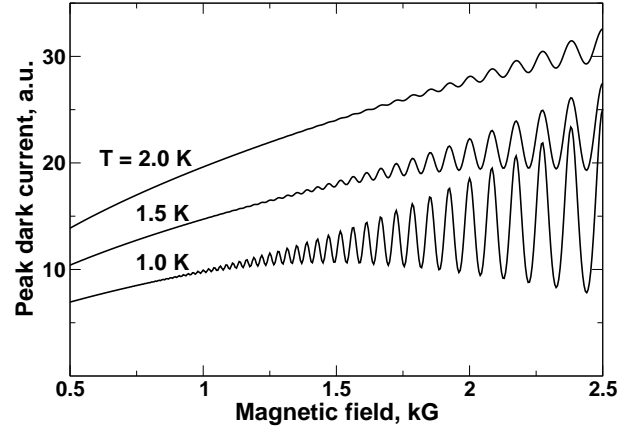


FIG. 4: Peak value of dark current vs magnetic field at different temperatures ($20 \leq \zeta/\hbar\Omega_c \leq 100$).

Here $\mu_2 \propto |C|^2 \sum_N f_N(1 - f_N)/\sqrt{N}$. One can see that the phonon distribution function is excluded from the expression for the dissipative current. This is because the contributions of the processes of the stimulated emission of phonons and their absorption compensate each other in the intra-LL transitions (see Fig. 2). Further integration in the right-hand side of Eq. (6) over q_{\perp} and Φ yields

$$j_2 = \frac{\sqrt{\pi} \mu_2 \hbar s}{2\sqrt{2}eL^2} \int_0^{\sqrt{F^2-1}/F} \frac{d \cos \Phi}{\sqrt{(F^2-1) - F^2 \cos^2 \Phi}} \times \frac{1}{\sqrt{1 + a^2(F^2-1) - a^2 F^2 \cos^2 \Phi}} \simeq \frac{\pi^{3/2} \mu_2 \hbar s}{2^{5/2} e L^2} \frac{1}{F} \quad (7)$$

with $a = l/L \ll 1$.

Taking into account Eqs. (1), (3), and (7), we arrive at the following current-voltage characteristic:

$$j_d(E) = \sigma_1 E + \frac{\pi^{3/2} \mu_2}{2^{5/2}} \frac{E_s^2}{E} \Theta(E - E_s), \quad (8)$$

where $\Theta(E)$ is the unity-step function, which in the case of marked LL broadening should be replaced by a smoother function. Figure 3 shows the dark current-voltage characteristics calculated using the above formulas. It exhibits a pronounced overshoot of the dark current. The electric-field dependence of the dissipative conductivity (with a jump at $E \simeq E_s$) similar to that following from Eq. (8) was recalculated from the experimental data at rather strong magnetic field [28] and, consequently, proportionally large E_s (see also Ref. [29]).

As follows from the obtained expressions, the dissipative current at $E > E_s$ depends on the temperature only via the factor μ_2 . This factor provides a nontrivial dependence of the dissipative conductivity, particularly at its peak magnitude, on the magnetic field. Figure 4 shows the peak value (at $E = E_s$) of the dissipative current as a function of the magnetic field. The pronounced

oscillations in Fig. 4 are akin to the Shubnikov-de Haas oscillations.

The relative height of the current overshoot is given by

$$\left. \frac{j_2}{j_1} \right|_{E=E_s} \simeq \left(\frac{\mu_2}{\mu_1} \right) \left(\frac{T}{ms^2} \right) \exp \left(\frac{\hbar\Omega_c}{T} \right) \gg 1. \quad (9)$$

The ratio μ_2/μ_1 varies with the magnetic field because the LL filling factor depends on the LL positions with respect to the Fermi level. However, when $T < \hbar\Omega_c$, the product $(\mu_2/\mu_1) \exp(\hbar\Omega_c/T) \gg 1$ at all values of $(\zeta - N_m \hbar\Omega_c)$. The parameter T/ms^2 exceeds unity at $T > 50$ mK.

A sharp increase in the dissipative current at $E = E_s$ can also occur due to the electron interaction with interface acoustic phonons. In this case, owing to specific electron-phonon scattering selection rules [30], the dissipative current can reveal even sharper overshoot at $E = E_s$.

Because of a strong overshoot of the dissipative dark current at $E = E_s$, the net dissipative conductivity of a 2DES irradiated with microwaves can change its sign at $E_0 \simeq E_s$. The net current voltage characteristic of a 2DES under microwave irradiation with $\sigma_{ph} < 0$ (associated, for example, with the photon-assisted scattering on impurities) is shown schematically in the inset in Fig. 3. The latter characteristic corresponds to an abrupt change in the sign of the net dissipative conductivity, i.e., the breakdown of ANC, at $E_0 \simeq 3$ V/cm. A sharp transition from $\sigma(E) < 0$ at $E < E_0 \simeq E_s$ to $\sigma(E) > 0$ when E exceeds E_s can significantly influence the domain structures resulting in ZR and ZC states. The remarkable feature of these domain structures is that the regions, where $E_x > E_s$ in the Hall bar configuration or $E_y > E_s$ in the Corbino samples, shown in Fig. 1 by the shaded “lanes” with arrows, are sources of the acoustic phonons

generated by the electron streams with supersonic Hall drift velocities. The generation of acoustic phonons by these streams can lead to a pronounced deviation of the phonon system from equilibrium. This, in turn, can affect the values and sign of the dissipative conductivity [15].

Worth noting the feasibility of formation of stable ZR states at relatively large currents. These states can correspond to $\langle E_x \rangle \simeq \pm E_0$ when the electric-field distributions are nearly uniform. The states in question can be formed when $J_y \simeq \pm J_0 = \pm \sigma_H d E_0$. Taking into account that $\sigma_H = ec\Sigma/H$, where Σ is the electron sheet concentration, and assuming $E_0 = E_s$, one can obtain $J_0 \simeq esd\Sigma$. The quantity J_0 is by two orders of magnitude larger than the currents in ZR states observed experimentally. The states with smooth electric-field distributions can arise in the Corbino samples at the applied voltage $V_y \simeq \pm V_0$ with $V_0 = dE_0 \simeq \pm dE_s$. If $d = 0.25$ cm, at $H = 1$ kG one obtains $V_0 \simeq 0.75$ V. Due to the absence of dissipation, the Joule heating can be disregarded despite relatively large values of the current (applied voltage).

In summary, we calculated the electric-field dependence of the dissipative dark current associated with the scattering of electrons on acoustic phonons in a 2DES subjected to a magnetic field. The obtained current-voltage characteristic exhibits a strong overshoot at a certain electric field. This field corresponds to the Hall drift velocity equal to the speed of sound. The overshoot of the dark component of the dissipative current can suppress the negative microwave photoconductivity (breakdown of ANC) in the regions with high electric field, where supersonic electron streams occur, and affect the formation of domain structures with the zeroth resistance/conductance.

The authors thank V. Volkov and V. Vyurkov for fruitful discussions and comments on the manuscript.

-
- [1] R. G. Mani, J. H. Smet, K. von Klitzing, V. Narayana-murti, W. B. Johnson, and V. Umansky, *Nature* **420**, 646 (2002).
 - [2] M. A. Zudov, R. R. Du, L. N. Pfeiffer, and K. W. West, *Phys. Rev. Lett.* **90**, 046807-1, (2003).
 - [3] C. L. Yang, M. A. Zudov, T. A. Knuuttila, R.R.Du, L. N. Pfeiffer, and K. W. West, *cond-mat/0303472* (2003).
 - [4] P. W. Anderson and W. F. Brinkman, *cond-mat/0302129* (2003).
 - [5] A. V. Andreev, I. L. Aleiner, and A. J. Millis, *cond-mat/0302063* (2003).
 - [6] F. S. Bergeret, B. Huckestein and A. F. Volkov, *cond-mat/0303530* (2003).
 - [7] V. I. Ryzhii, *Fiz. Tverd. Tela* **11**, 2577 (1969) [*Sov. Phys.-Solid State* **11**, 2078 (1970)].
 - [8] V. I. Ryzhii, R. A. Suris, and B. S. Shchamkhalova, *Fiz. Tekh. Poluprovodn.* **20**, 2078 (1986) [*Sov. Phys.-Semicond.* **20**, 1299 (1986)].
 - [9] A. C. Durst, S. Sachdev, N. Read, and S. M. Girvin, *cond-mat/0301569* (2003).
 - [10] X. L. Lei and S. Y. Liu, *cond-mat/03004687* (2003).
 - [11] M. G. Vavilov and I. L. Aleiner, *cond-mat/03005478* (2003).
 - [12] V. Shikin, *JETP Lett.* **77**, 236 (2003).
 - [13] V. Ryzhii and V. Vyurkov, *cond-mat/0305199* (2003).
 - [14] V. Ryzhii, *cond-mat/0305454* (2003).
 - [15] V. Ryzhii, *cond-mat/0305484* (2003).
 - [16] R. Klesse and F. Merz, *cond-mat/0305492* (2003).
 - [17] A. F. Volkov and V. V. Pavlovskii, *cond-mat/0305562* (2003).
 - [18] B. A. Tavger and M. Sh. Erukhimov, *Zh. Eksp. Teor. Fiz.* **51**, 528 (1966) [*Sov. Phys. JETP* **24** 354 (1967)].
 - [19] V. I. Ryzhii, *Fiz. Tekh. Poluprovodn.* **3**, 1704 (1969) [*Sov. Phys.-Semicond.* **3**, 1704 (1969)].
 - [20] V. L. Pokrovsky, L. P. Pryadko, and A. L. Talapov, *J. Phys.: Cond. Mat.* **2**, 1583 (1990).
 - [21] M. Sh. Erukhimov, *Fiz. Tekh. Poluprovodn.* **3**, 194 (1969)

- [Sov. Phys.-Semicond. **3**, 162 (1969)].
- [22] P. Streda and K. von Klitzing, J. Phys. C **17**, L483 (1984).
 - [23] O. Heinonen, P. L. Taylor, and S. M. Girvin, Phys. Rev. B **30**, 3016 (1984).
 - [24] P. Streda, J. Phys. C **19**, L155 (1986).
 - [25] O. G. Balev, Fiz. Tverd. Tela **32**, 871 (1990) [Sov. Phys.-Solid State **32**, 514 (1990)].
 - [26] C. Chaubet, A. Raymond, and D. Dur, Phys. Rev. B **52**, 11178 (1995).
 - [27] G. Nachtwei, Physica E, **4**, 79 (1999).
 - [28] S. Komiyama and Y. Kawaguchi, Phys. Rev. B **61**, 2014 (2000).
 - [29] B. E. Sagol, G. Nachtwei, K. von Klitzing, G. Hein, and K. Eberl, Phys. Rev. B **66**, 075305-1 (2002).
 - [30] C. L. Yang, J. Zhang, R. R. Du, J. A. Simmons, and J. L. Reno, Phys. Rev. Lett. **89**, 076801-1 (2002).